RBFTA
Revista Brasileira de Física Tecnológica Aplicada
ISSN: 2358-0089

https://periodicos.utfpr.edu.br/rbfta

Impedance spectroscopy in asphaltene-toluene and maltene-toluene solutions of crude oils from the Orinoco Belt

José Antonio Navia
naviajosea@gmail.com
orcid.org/0000-0001-3752-7298
Universidad Central de Venezuela (UCV), Ciudad Universitaria, Caracas, Venezuela.

David Oliva
avilod12@gmail.com
orcid.org/0000-0002-5615-3960
Universidad Central de Venezuela (UCV), Ciudad Universitaria, Caracas, Venezuela.

José Jorge
josejorgea@gmail.com
orcid.org/0000-0002-9893-1748
Universidad Central de Venezuela (UCV), Ciudad Universitaria, Caracas, Venezuela.

ABSTRACT

In this investigation, an impedance and dielectric spectroscopy study was carried out on Asphaltene-Toluene and Maltene-Toluene solutions, prepared from two oil samples from the Orinoco Oil Belt that presented low resistivity at the depths of the oil well where petrophysical logs were taken. The purpose of this work is to investigate whether the asphaltenes and maltenes would be responsible for the low resistivities found in the logs. A Lock-In amplifier, an impedance analyzer, and a coaxial cylindrical cell were used to obtain the impedance measurements. From the plotting of the impedance and phase angle parameters, it was confirmed Asphaltene-Toluene solutions were the least resistive. A fit of the experimental data based on an electrical circuit was realized, finding good correspondence between the experimental data and the fit line. The AC conductivity values were plotted using the fitting data, and it was observed that the Asphaltene-Toluene solution is more conductive. A remarkable difference in the electrical behavior was found between the maltene solutions of both crude oil samples.

KEYWORDS: spectroscopy; impedance; conductivity; solutions.

INTRODUCTION

Studying the physical-chemical properties of oil within oil industry is indispensable for planning, extracting, processing and commercialization (ROCHA et al., 2019). Nowadays, it is possible to apply new methods that allow a better characterization of crude oil (RODGERS; MCKENNA, 2011) and its components in a non-destructive and economic way; focusing on its dielectric properties (JORGE et al., 2018).

Electrochemical Impedance Spectroscopy (EIS) has been established as a simple and effective technique in the study of the electrical properties of materials (LVOVICH, 2012). It consists in applying an external alternate voltage $V = V_0\, e^{(j\omega t)}$ to a test sample, thus generating a current that is captured by a sensor. With both quantities, complex impedance (Z^*) is determined (JORGE et al., 2018). Other electrical properties derived from Z^* are electrical permittivity (ε^*) and conductivity (σ^*), both complex functions depending on angular frequency (KREMER; SCHÖNHALS, 2003).

Another technique, derived from EIS, dielectric spectroscopy (DS), considers the real (ε') and imaginary (ε'') parts of the electrical permittivity. ε' is also known as the dielectric constant and is related to the storage of electrical energy, ε'' is associated with electrical conduction (GOUAL, 2009; GERHARDT, 1994). Dielectric response to the external stimulus is based on electric energy storage and subsequent relaxation. Dielectric relaxation describes the time in which dipolar molecules re-align after the application of an external alternating electric field; as frequency increases, ε' decreases and ε'' increases given that polarization cannot align with the electric field at high frequencies. Large non-polar molecules lose their orientation with the field at low frequencies and have relaxation times (τ) in the order of seconds. Smaller ionic and polar species lose orientation between kHz and MHz and τ are between ms and μs (KREMER; SCHÖNHALS, 2003).

Dependence of ε^* with angular frequency is described through dielectric relaxation models. Debye's model is used for pure insulators and considers a single τ. The Cole-Cole model is used for dielectric materials with a greater molecular complexity and considers different polarization processes and a distribution of relaxation times. (LVOVICH, 2012; GERHARDT, 1994). Depending on the studied material, polarization can be: electronic and atomic (THz frequencies), dipole (kHz-MHz frequency) and ionic (Hz-kHz frequency) (KREMER; SCHÖNHALS, 2003).

Within the Cretaceous formation of the Temblador Group of the Orinoco Oil Belt, a sandy sequence saturated with heavy oil was found after dielectric and nuclear magnetic resonance registers were running in an oil well. This result contrasts with conventional logs taken in the same well, which showed low resistance and high radioactivity values, indicating the absence of oil (JAIMES et al., [s.d.]).

In this work, an EIS and DS study was carried out on two solutions of asphaltene in toluene and two solutions of maltene in toluene, from two crude oil samples from the Cretaceous formation of the Orinoco Oil Belt, as part of an investigation to determine the causes of the low resistivity (JORGE et al., 2018). Electric impedance and phase angle were measured in the range of 40 Hz to 10MHz, using an impedance analyzer, a lock-in amplifier, and a stainless steel

coaxial cylindrical cell. Electrical conductivity was determined from impedance. The experimental impedance data was fitted to an electrical circuit model that simulates the behavior of the solutions.

ELECTRICAL PROPERTIES

In the analysis of electrical properties of materials, complex functions such impedance (Z^*) with real (Z') and imaginary (Z'') parts; permittivity (ε^*), real (ε') and imaginary (ε'') parts; and conductivity (σ^*) with real (σ') and imaginary (σ'') parts are used. Specifically, Z^* is described by the following equation:

$$Z^* = \frac{V_{(t)}}{I_{(t)}} = \frac{V_0 e^{-j\omega t}}{I_0 e^{-j(\omega t+\theta)}} = |Z|e^{j\theta} = |Z|(\cos\theta + j\sin\theta) = Z' + jZ'' \quad (1)$$

where ω is the angular frequency, $|Z|$ is the impedance modulus and ϑ the phase angle between current and voltage and $j = \sqrt{-1}$.

Using impedance measurements and the geometric capacitance (C_0) of the capacitive sensor, the rest of the properties are obtained. Particularly, AC electrical conductivity, as a function of impedance, is described by the following equation:

$$\sigma' = \frac{\varepsilon_0 Z'}{|Z|^2 C_0} \quad (2)$$

ASPHALTENES AND MALTENES

Asphaltenes are defined as the most complex and heavy fraction of crude oil that is insoluble in light n-alkanes such as n-pentane or n-heptane, but soluble in aromatic compounds like toluene. They are the most polar compounds in crude oil due to the presence in their structure of polar functional groups such as sulfur, aldehyde, carbonyl, carboxylic, amine, amide, and some metals such as nickel, vanadium, and iron, making them the most conductive fraction of oil (SANDOVAL, 2011).

Maltenes are known as the portion of oil that is solubilized when it is dissolved in n-heptane but is adsorbed on a surface-active material, and are made up of three fractions of oil: saturate, aromatic and resins (ADEBIYI et al., 2016).

EXPERIMENTAL SECTION

Two extra-heavy oil samples, C1 and C2, from the Orinoco Oil Belt were used. Sample C1 dates from the Cretaceous and sample C2 from the Miocene. Physical properties of crude oil samples are shown in **Table 1**.

Table 1- Physical propierties of crude oil. Samples C1 and C2

Physical properties	C1	C2
Density at 50 °C (g/cm³)	0.9859	0.9916
Viscosity at 50 °C (cP)	16494	21590
API	8.67	8.10
% asphaltenes	15.10	7

Source: Own Authorship.

A SARA fractionation was performed on both samples, where 33 mg of asphaltenes and 288 mg of maltenes were obtained. Each fraction was added in different beakers with 40 ml of toluene and were stirred until a homogeneous solution was formed (NAVIA, 2019). The concentration of the solutions is shown in **Table 2**.

Table 2- Solutions content

Solutions	Solute mass (mg)	Volume solvent (ml)	[Kg/L]
Asphaltene-Toluene	33	40	$8.25x10^{-04}$
Maltene-Toluene	288	40	$7.20x10^{-03}$

Source: Own Authorship.

Impedance measurements were made in two frequency ranges. In the first one, from 40 Hz to 100 kHz, a lock-in amplifier model Standford Research Systems SR830 DSP was used. In the second range, from 100 kHz to 10 MHz, an HP 4192A LF Impedance Analyzer was used (ALBERTINI; KLEEMANN, 1997; NAVIA, 2019).

A coaxial cylinder stainless steel capacitor with Teflon covers was crafted as a capacitive sensor as shown in **Figure 1**. The geometry was selected with the aim of covering the widest possible frequency range (FOLGUERØ, 1998).

This capacitor is made up of two coaxial cylinders with an internal radius of 0.595 cm ± 0.005 cm, an external radius of 1.28 cm ± 0.005 cm and a height of 8.67 cm ± 0.005 cm. The geometric capacitance (C_0) was calculated from the equation:

$$C_0 = \frac{2\pi l \varepsilon_0}{\ln\left(\frac{r_2}{r_1}\right)} \tag{3}$$

where ε_0 is the vacuum permittivity. The value of C_0 is 6.29pF ± 0.01%.

Figure 1 – Coaxial cylinder cell seen from various positions: (A) Full cell ready to use, (B) cell without top cover, (C) cell with top cover

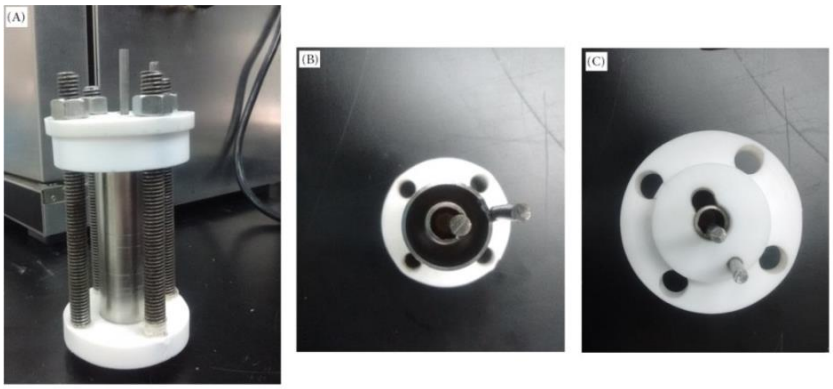

Source: Own Authorship.

RESULTS AND ANALYSIS

CELL CALIBRATION

Figure 2 shows the impedance modulus and phase angle of the measuring cell as a function of frequency for a range between 40 kHz and 10 MHz. The cell behaves like an ideal capacitor up to a frequency of 5 MHz. $|Z|$ decays as $1/\omega Co$ and ϑ is approximately $-\pi/2$. Above 5 MHz the angle begins to increase due to the impedance coupling between the cell and the analyzer.

Figure 2 - Bode diagrams of the empty cell

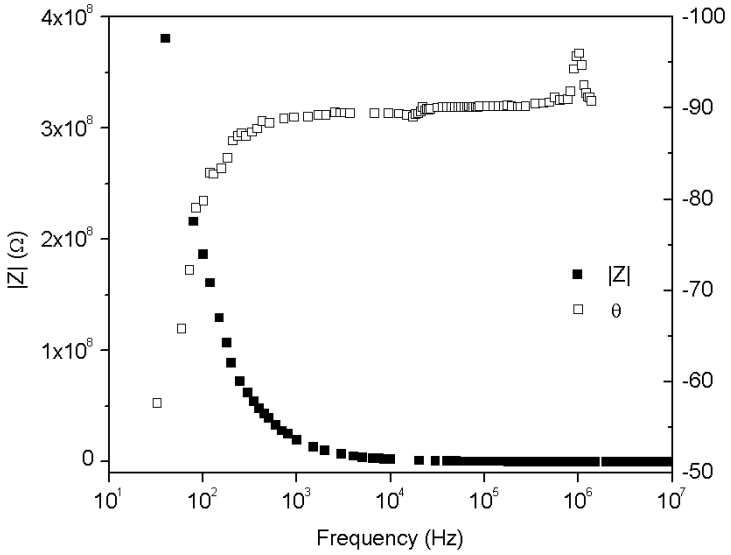

Source: Own Authorship.

BODE DIAGRAMS

Comparison between $|Z|$ and ϑ of asphaltene and maltene solutions is shown in **Figure 3**. In **Figure 3-A**, it can be seen that $|Z|$ of the asphaltene solution of crude oil C2 tends to be slightly higher than that of crude oil C1 up to 800 Hz, for higher frequencies the values tend to match. The phase angle diagram shows that the asphaltene solution C2 reaches the value of $-\pi/2$ faster than the solution C1.

In **Figure 3-B**, $|Z|$ of the maltene solution is plotted, where a difference between both curves is observed, being the solution of the C1 oil the one with the highest value of $|Z|$ at low frequencies compared to C2. This suggests that the chemical structure of the maltenes is different. In the phase bode diagram, the solution of maltene C1 tends first to $-\pi/2$ that the solution of C2.

CIRCUIT MODEL, CONDUCTIVITY AND IMAGINARY IMPEDANCE

Experimental data was fitted to a typical electrical circuit model for aqueous, conductive, and ionic solutions, known as Randles circuit. It is composed of a

resistance (*Rs*) in series with another resistance (*Rp*) in parallel with a capacitor (*Cp*), as shown in **Figure 4** (LVOVICH, 2012).

Rp represents the resistance of the medium to conduct charge carriers (conductivity of asphaltenes). It is related to the minimum voltage necessary for conductivity to occur and is the circuit element that dominates the system impedance when the frequency is on the order of Hz and mHz. *Cp* is the equivalent capacitance that is generated between the cell's electrodes and the adsorbed molecules on the surface of these as consequence of charge difference (isolation of non-conductive asphaltenes). This phenomenon occurs between 100 Hz and 1000 Hz. Finally, *Rs* corresponds to the volumetric resistance of the solution (Toluene Dissipation) (LVOVICH, 2012; GOUAL, 2009).

Figure 3 - $|Z|$ and ϑ as a function of frequency for asphaltene-toluene (A) and maltene-toluene (B) solutions of C1 and C2 samples

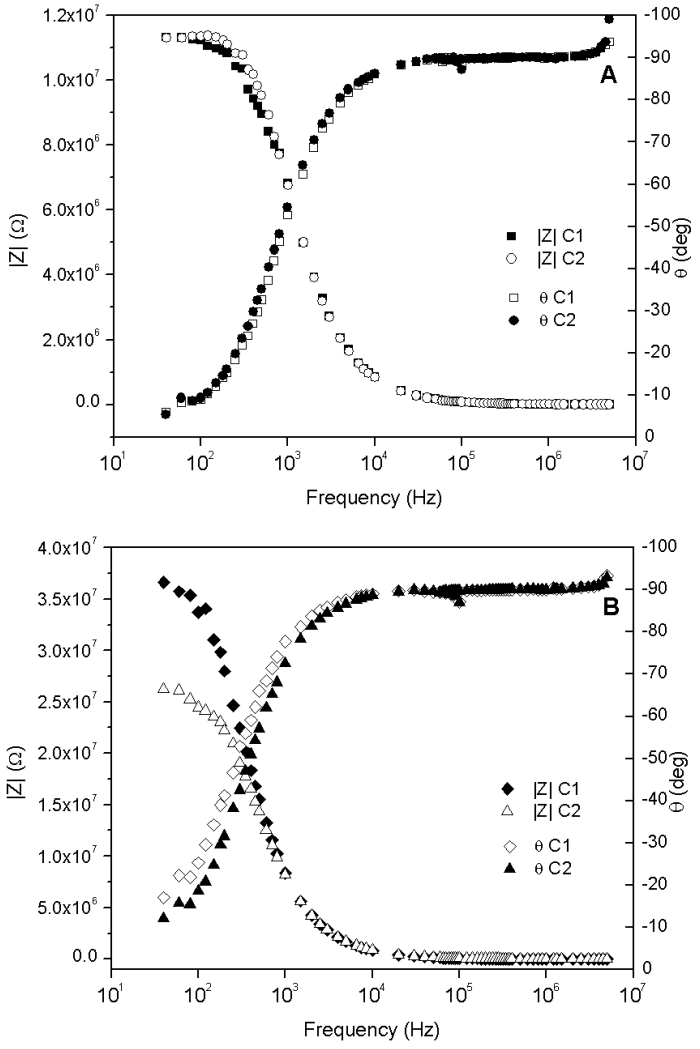

Source: Own Authorship.

Figure 4 - Electrical circuit model. Resistance Rs in series with parallel RC (Rp, Cp) circuit

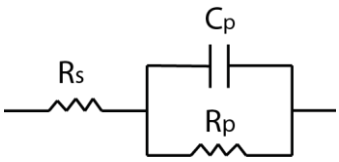

Source: GOUAL, 2009.

In **Figure 5** is shown the Nyquist diagram for asphaltene and maltene solutions of crude oil samples C1 and C2 with their correspondent fit line. A semicircle is seen for both asphaltene and maltene solutions, with a partial one for maltenes.

The presence of a single semicircle in the Nyquist diagram indicates a single relaxation process. The partial semicircle seen in maltenes implies a relatively less strong relaxation because of lower polarity in the maltenes (low dipole moment) (GOUAL, 2009). In each semicircle a good correspondence between experimental points and fit lines with minimal dispersion is found. It is also observed that both asphaltene samples are similar, while those of maltenes exhibit a pronounced difference.

Figure 5 - Nyquist diagrams for Asphaltene-Toluene and Maltene-Toluene solutions of C1 and C2 samples, with their respective fitting line

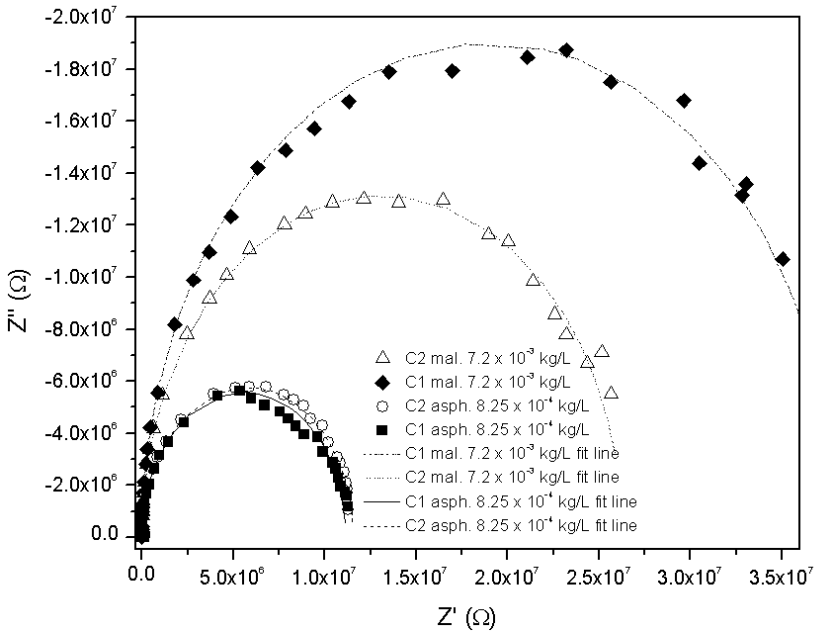

Source: Own Authorship.

Normalized imaginary impedance as function of frequency is presented in **Figure 6**. Four notable peaks are found at low frequencies, as shown in **Table 3**. Sample C1 asphaltenes show a peak at 800 Hz, maltenes at 250 Hz. Sample C2 asphaltenes peak is found at 700 Hz and maltenes at 350 Hz. These peaks are characteristic of relaxation processes. Given that maltenes have a low dipole moment the frequency of occurrence of maximum peak – critical frequency (*fc*) – is in the low frequency range, compared to asphaltenes (GOUAL, 2009). The

presence of a single maximum in the imaginary impedance graph indicates the existence of a single τ (LVOVICH, 2012).

Figure 6 - Normalized imaginary impedance of asphaltene and maltene

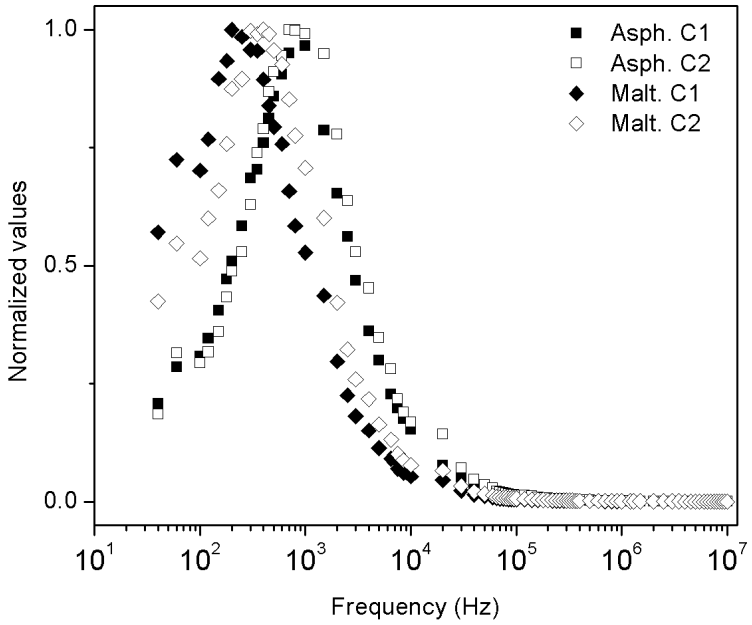

Source: Own Authorship.

Table 3- Occurrence frequency of peaks in imaginary impedance

	Solutions	Frequency of the peak *fc* (Hz)
Sample C1	**Asphaltene - Toluene**	800
	Maltene - Toluene	250
Sample C2	**Asphaltene - Toluene**	700
	Maltene - Toluene	350

Source: Own Authorship.

To calculate *fc*, *Rp* and *Cp* values were taken from fitting (**Table 5**) and used in the following equation:

$$f_c = \frac{1}{2\pi R_p C_p} \quad (4)$$

The sample C1 asphaltene solution's calculated *fc* was of 809.90 Hz and the maltene solution was of 235.64 Hz, while the asphaltene solution of sample C2 was of 749.54 Hz and the maltene solution was of 329.38 Hz. All *fc* calculated values are shown in **Table 4**.

Table 4- Critical frequency of peaks in imaginary impedance from model

	Solutions	Calculated *fc* (Hz)
Sample C1	**Asphaltene - Toluene**	809.90 ± 20
	Maltene - Toluene	235.64 ± 9
Sample C2	**Asphaltene - Toluene**	749.54 ± 20
	Maltene - Toluene	329.38 ± 5

Source: Own Authorship.

Experimental AC conductivity values are plotted as function of frequency in **Figure 7**, following **Equation 2**. It is observed that the asphaltene solution of sample C1 shows a slightly higher conductivity than the one of sample C2. The maltene solution of sample C2 is seen to be more conductive than that of sample C1. In general, both maltene solutions are less conductive than asphaltene solutions.

AC conductivity from *Rs*, *Rp* and *Cp* fitting values was determined. Obtained values can be seen in **Table 5**.

Figure 7 - AC conductivity for asphaltene-toluene and maltene-toluene solutions of C1 and C2 samples

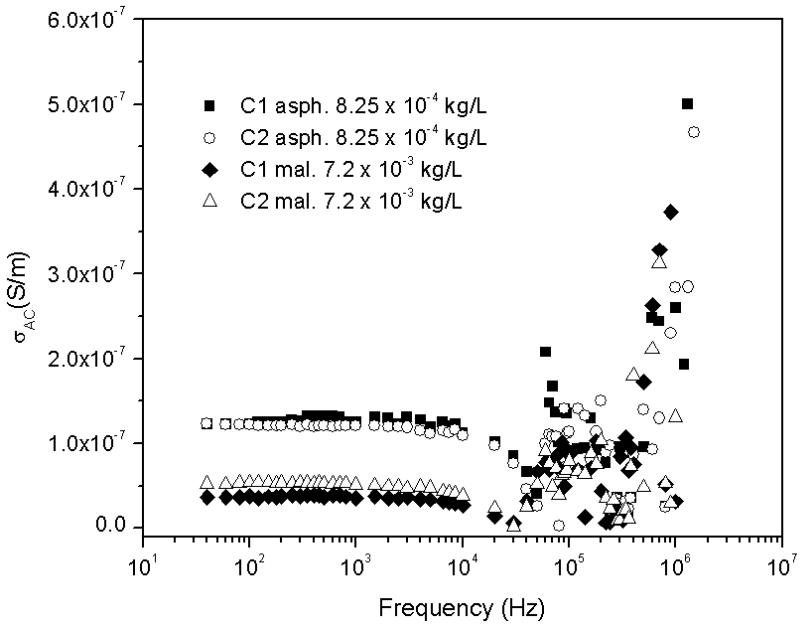

Source: Own Authorship

Table 5 - Values of circuit model from the fit to experimental data

	C1			C2		
	Elements of the circuit model					
	Rs (Ω)	Rp (MΩ)	Cp (pF)	Rs (Ω)	Rp (MΩ)	Cp (pF)
Asphaltene - Toluene	7.19±2%	11.14±1.7%	17.64±0.8%	10±4%	11.54±1.8%	18.4±0.9%
Maltene - Toluene	10±4.7%	37.69±2.6%	17.92±1.3%	10±5.3%	26.26±1%	18.4±0.4%

Source: Own Authorship

AC conductivity from fitting is determined by equations (GOUAL, 2009):

$$\sigma'_{AC} = \left(\frac{1}{C_0}\right)\frac{R_p+R_s+\omega^2 R_s R_p^2 C_p^2}{(R_p+R_s)^2+(\omega R_s R_p C_p)^2} \quad (5)$$

$$\sigma'_{DC} = \left(\frac{1}{C_0}\right)\frac{1}{R_p+R_s} \quad (6)$$

Behavior of AC conductivity from fitting (**Equation 5**) is shown in **Figure 8**. Asphaltene solutions are the ones with higher conductivity compared to maltene solutions, being the asphaltene of sample C1 the most conductive. Maltene solution of C2, once again, is more conductive than that of C1.

AC conductivity from fitting remains constant up to 700 kHz and increases strongly at higher frequencies. Asphaltene solutions show high AC and DC conductivity values, as seen in **Table 6**, being the solution of sample C1 the most conductive given that is has the highest content of asphaltenes. In other works, it was found that conductivity increases with asphaltene concentration, temperature, and solvent dielectric constant (GOUAL, 2009).

Figure 8 - AC conductivity for asphaltene-toluene and maltene-toluene solutions of C1 and C2 crudes from fitting to experimental data

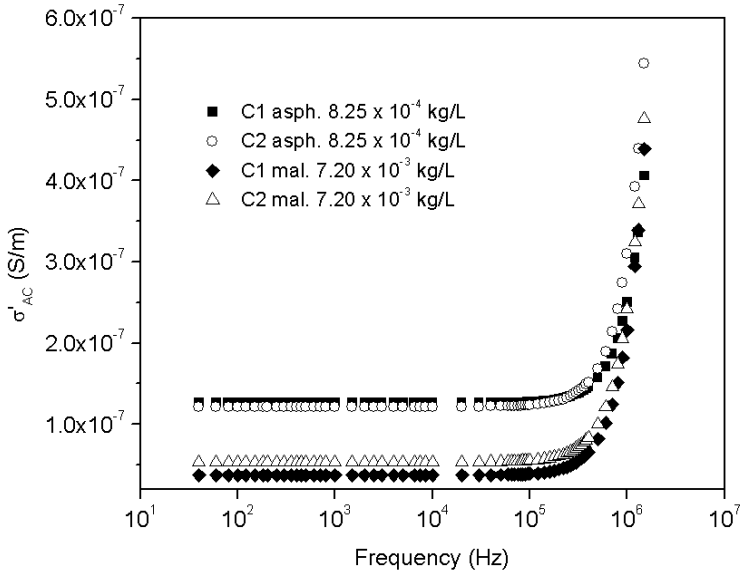

Source: Own Authorship.

Table 6 - DC conductivity obtained from fitting to experimental data

Solutions	(σ_{DC} ±0.001%) (S/m)		(σ_{AC} at 40 Hz ±0.001%) (S/m)	
	Crude oil C1	Crude oil C2	Crude oil C1	Crude oil C2
Asphaltene - Toluene	$1.26x10^{-07}$	$1.21x10^{-07}$	$1.26x10^{-07}$	$1.21x10^{-07}$
Maltene - Toluene	$3.73x10^{-08}$	$5.35x10^{-08}$	$3.73x10^{-08}$	$5.35x10^{-08}$

Source: Own Authorship.

CONCLUSION

Impedance values of both asphaltene solutions are similar at low frequencies while the maltene solution of sample C1 is higher than that of sample C2 due to the distribution of the remaining crude oil fractions (aromatic, resins and saturated).

All solutions present a single relaxation mechanism and a single relaxation time as it was noticed in the Nyquist diagrams. Partial semicircle in maltene solutions is due to a less strong relaxation process.

The *Z''* graph for all solutions show a characteristic peak at low frequencies. The asphaltene solution of sample C1 has a higher *fc* than the one of sample C2 while the maltene solution of sample C2 is higher than that of sample C1. *fc* calculated from fitting coincide with experimental *fc* obtained from *Z''*.

Experimental AC conductivity showed that asphaltene solutions are more conductive than maltene solutions, thus making the C1 oil more conductive than C2 oil given that it has a higher amount of asphaltenes. Maltene solution of sample C2 has a higher conductivity than the solution of sample C1.

AC conductivity from fitting show the same behavior as experimental AC conductivity. It was found once again that asphaltene solutions are more conductive than maltene solutions and the maltene solution from sample C2 is more conductive than the solution of sample C1.

DC conductivity, experimental and from fitting, and AC conductivity of asphaltenes and maltenes solutions at low frequencies are the same for both crude oil samples.

Electrical impedance and conductivity are similar in the asphaltene solutions of both samples while in maltene solutions there is a noticeable difference.

Espectroscopia de impedância em soluções de Asfalteno-Tolueno e Malteno-Tolueno de óleos do Cinturão Petrolífero do Orinoco

RESUMO

Neste artigo, foi realizado um estudo de impedância e espectroscopia dielétrica em soluções de Asfalteno-Tolueno e Malteno-Tolueno, preparado a partir de duas amostras de petróleo bruto do Cinturão petrolífero do Orinoco que mostraram baixa resistividade nas profundidades dos poços onde os registros petrofísicos foram levados. O objetivo deste trabalho é investigar se os asfaltenos e os maltenos, componentes destes óleos brutos, são responsáveis pelas baixas resistividades encontradas nos registros convencionais. Para obter as medidas de impedância, foram utilizados um amplificador Lock-In, um analisador de impedância e uma célula cilíndrica coaxial. A partir do traçado dos parâmetros de impedância e ângulo de fase, foi confirmado que as soluções de Asfalteno-Tolueno eram as menos resistivas. Um ajuste dos dados experimentais baseado em um circuito elétrico foi realizado; uma boa correspondência foi encontrada entre os valores experimentais e a linha de ajuste. Os valores de condutividade AC foram traçados utilizando os dados ajustados, mostrando que a solução asfalteno-Tolueno é mais condutiva. Uma diferença notável foi encontrada no comportamento elétrico entre as soluções de malteno dos dois óleos brutos

PALAVRAS-CHAVE: espectroscopia; impedância; condutividade; soluções.

Espectroscopía de impedancia en soluciones asfalteno-tolueno y malteno-tolueno de crudos de la Faja Petrolífera del Orinoco

RESUMEN

En la presente investigación, se llevó a cabo un estudio de espectroscopía de impedancia y dieléctrica en soluciones de Asfalteno-Tolueno y Malteno-Tolueno, preparadas a partir de dos crudos provenientes de la Faja Petrolífera del Orinoco que presentaban baja resistividad en las profundidades del pozo donde fueron tomados los registros petrofísicos. La finalidad de este trabajo, es investigar si los asfáltenos y los maltenos, componentes de estos crudos, serían los responsables de las bajas resistividades encontradas en los registros convencionales. Para la obtención de las medidas de impedancia se utilizó un amplificador Lock-In, un analizador de impedancia y una celda cilíndrica coaxial. A partir de la graficación de los parámetros de impedancia y ángulo de fase, se confirmó que las soluciones de Asfalteno-Tolueno fueron las menos resistivas. Se realizó un ajuste de los datos experimentales basado en un circuito eléctrico; encontrándose buena correspondencia entre los valores experimentales y la línea de ajuste. Se graficaron los valores de conductividad AC utilizando los datos del ajuste realizado, observándose que, la solución de Asfalteno-Tolueno es más conductiva. Se encontró una diferencia notable en el comportamiento eléctrico entre las soluciones de maltenos de los dos crudos.

PALABRAS CLAVE: espectroscopía, impedancia, conductividad, soluciones.

REFERÊNCIAS

ADEBIYI, F. M. et al. Spectroscopic Characterization of the Maltene Fraction of Nigerian Bitumen for Potencial Health-Risk Assessment. **Energy Sources, Part A: Recovery, Utilization and Environmental Effects**, v. 38, n. 16, p. 2397-2405, 2016.

ALBERTINI, A.; KLEEMANN, W. Analogue and Digital Lock-In Techniques for Very-Low-Frequency Impedance Spectroscopy. **Measurement Science and Technology**, v. 8, n. 6, p. 666-672, 1997.

FOLGERØ, K. Broad-Band Dielectric Spectroscopy of Low-Permitivity Fluids Using One Measurement Cell. **IEEE Transaccions on Instrumentation and Measurement**, v. 47, n. 4, p. 881-885, 1998.

GERHARDT, R. Impedance and Dielectric Revisited: Distinguishing From Long-Range Conductivity. **Journal of Physical and Chemistry of Solids**, v. 55, n. 12, p. 1491-1506, 1994.

GOUAL, L. Impedance Spectroscopy of Petroleum Fluids at low frequency. **Energy and Fuels**, v.23, n. 4, p. 2090-2094, 2009.

JAIMES, G. et al. Aplicación de Nuevas tecnologías para la detección de Crudos Pesados de baja Resistividad y Alta radioactividad en el Campo Dobokubi de la Faja Petrolífera del Orinoco. P. 1-10, [s.d.].

JORGE, J. et al. Espectroscopía de Impedancia en Crudos de la Cuenca Apure-Barinas y la Faja Petrolífera del Orinoco en un Rango de Frecuencias Intermedias. **Revista de la Facultad de Ingeniería. Universidad Central de Venezuela**, v. 33, n. 2, p. 49-58, 2018.

JORGE, J. et al. Impedance Spectroscopy in water/oil Emulsions in a Range of Intermediate Frequencies. **Revista Ingeniería UC**, v. 25, n. 3, p. 388-395, 2018.

KREMER, F.; SCHÖNHALS, A. **Broadband Dielectric Spectroscopy**. Berlin, Heidleberg, New York: Springer-Verlag, 2003.

LVOVICH, V. F. **Impedance Spectroscopy: Applications to Electrochemical and Dielectric Phenomena**, New Jersey: John Wiley & Sons, Inc, 2012.

NAVIA, J. **Espectroscopía de Impedancia en Soluciones Asfalteno-Tolueno y Malteno-Tolueno de Crudos de la Faja Petrolífera del Orinoco**, Undergraduate Thesis: Universidad Central de Venezuela, 2019.

ROCHA, J. W. S. et al. Investigation of Electrical Properties with Medium and Heavy Brazilian Crude Oils by Electrochemical Impedance Spectroscopy. **Fuel**, v. 241, n. August 2018, p. 42-52, 2019.

RODGERS, R.P.; MCKENNA, A. M. Petroleum Analysis. **Analytical Chemistry**, v.83, n. 12, p. 4665-4687, 2011.

SANDOVAL, K. **Determinación de la Importancia de los Compuestos Atrapados en las Propiedades de los Asfaltenos**, Undergraduate Thesis: Universidad Central

Recebido: 06 de dezembro de 2020.
Aprovado: 11 de janeiro de 2022.

DOI:

Como citar: NAVIA, J A, OLIVA, D J, ALVIAREZ, J J , Impedance spectroscopy in asphaltene-toluene and maltene-toluene solutions of crude oils from the Orinoco Belt, **Revista Brasileira de Física Tecnológica Aplicada**, Ponta Grossa, v. 9, n. 1, p. 1-15, jan. 2022.

Contato: Jose Antonio Navia: naviajosea@gmail.com